Journal of Alloys and Compounds 509 (2011) 6666–6672

Contents lists available at ScienceDirect

Journal of Alloys and Compounds

journal homepage: www.elsevier.com/locate/jallcom

Evolution of Ag_3Sn at Sn–3.0Ag–0.3Cu–0.05Cr/Cu joint interfaces during thermal aging

Fei Lin[a,*], Wenzhen Bi[a], Guokui Ju[a], Wurong Wang[a], Xicheng Wei[a,b,*]

[a] School of Materials Science and Engineering, Shanghai University, Shanghai 200072, China
[b] Key State Lab for New Displays and System Integration (Chinese Ministry of Education), Shanghai 200072, China

ARTICLE INFO

Article history:
Received 16 November 2010
Received in revised form 18 March 2011
Accepted 23 March 2011
Available online 1 April 2011

Keywords:
Ag_3Sn
Aging
Sn–3.0Ag–0.3Cu–0.05Cr/Cu joint
Intermetallic compounds (IMC)

ABSTRACT

The intermetallic compounds (IMC) in the solder and at the interface of Sn–3.0Ag–0.5Cu (SAC)/Cu and Sn–3.0Ag–0.3Cu–0.05Cr (SACC)/Cu joints were investigated after isothermal aging at 150 °C for 0, 168 and 500 h. Different shaped Ag_3Sn phases were found near the IMC layer of the latter joint. Interestingly, fine rod-shaped and branch-like Ag_3Sn were detected near the interface after soldering and long Ag_3Sn changed into shorter rods and small particles during aging. It is investigated that the Cr addition and thermal aging have effect on the evolution of Ag_3Sn morphologies and it is controlled by interfacial diffusion. Energy minimization theory and the redistribution of elements are used to explain the morphological evolution of Ag_3Sn. Small Ag_3Sn particles were also found on the IMC layer after aging, unlike the large Ag_3Sn at that of SAC/Cu joints. In conclusion, a favorable morphology of the joint interface leads to better bonding properties for SACC/Cu joints against thermal aging than that for SAC/Cu.

© 2011 Elsevier B.V. All rights reserved.

1. Introduction

Solder plays a crucial role in the assembly and interconnection of electronic products. As a joint material, solder provides electronic, thermal and mechanical continuity [1]. Primarily, it should wet the substrate and provide good adhesion. With the inevitable trend to implement lead-free soldering due to environmental and health concerns, soldering reactions have been extensively studied during the last few decades [2–4]. The core issue is the formation and growth of intermetallic compounds (IMC) between the solder and the substrate.

Due to its good mechanical properties, adequate wetting characteristics as well as the comparable melting temperature, Sn–3.0Ag–0.5Cu (SAC) solder alloy has become one of the most important candidates replacing lead-tin solder. Concerning the microstructure of SAC solder, it is a mixture of Sn and IMC, such as Ag_3Sn and Cu_6Sn_5. The survey literature [5] showed that three types of Ag_3Sn compounds during solidification at different cooling rates are found to be particle-like, needle-like and plate-like. The mechanical properties of solder will be anisotropic when the IMC dispersion in Sn matrix is inhomogeneous [3]. If large Ag_3Sn plates form at the stress concentration region, cracks can initiate and propagate along the interface between the Ag_3Sn and the solder, which deteriorate the reliability of solder joint. Kim et al. [4] reported that the formation of large Ag_3Sn could be attributed to the solder composition and there was little effect from substrates. They observed large Ag_3Sn for high Ag content solder joints, the shapes of which were dendrite-like and hopper crystal-like plates. The formation sites of large Ag_3Sn plates were at the top of the interfacial reaction layer and the voids.

However, fine Ag_3Sn precipitates can pin the grain boundaries in the solder, stabilize the microstructure and strengthen the matrix [6]. Ag_3Sn particles could be evenly distributed among the eutectic or along the Sn-rich phase boundary in SnAgCu systems [7]. During high-temperature aging, Ag_3Sn with a large aspect ratio would experience the process of breakdown and surface spheroidization to form smaller aspect ratio Ag_3Sn [8,9]. Interestingly, nano-Ag_3Sn particles were discovered on the surface of IMC, and the existence of these particles would decrease the interfacial energy and hamper the growth of Cu_6Sn_5 IMC layer [10–12]. Obviously, it is of interests to understand the morphological evolution of Ag_3Sn in lead-free solder joints, especially near the IMC layer during reflow soldering and isothermal aging.

Our previous study [13] found that the trace of Cr addition observably reduced the growth rate of IMC layer and affected its shape at the interface of Sn–3.0Ag–0.3Cu–0.05Cr (SACC)/Cu joint. Meanwhile, short rod-shaped and small Ag_3Sn particles were present near the IMC layer of SACC/Cu joint, which might evolve from the long Ag_3Sn during aging. It is anticipated that the microstructural evolution significantly influences the reliability of

* Corresponding authors at: School of Materials Science and Engineering, Shanghai University, Shanghai 200072, China. Tel.: +86 021 56331377; fax: +86 021 56331466.
E-mail address: wxc1028@staff.shu.edu.cn (X. Wei).

0925-8388/$ – see front matter © 2011 Elsevier B.V. All rights reserved.
doi:10.1016/j.jallcom.2011.03.134

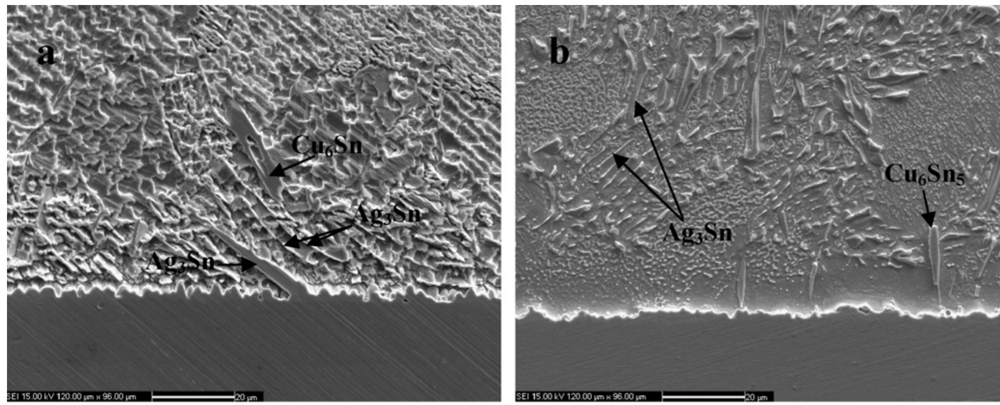

Fig. 1. SEM images of SAC/Cu (a) and SACC/Cu (b) joints after reflow soldering.

solder joints. Therefore, to provide useful information for reliability evaluations of solder joints, the present work focuses on the evolution of Ag_3Sn and discusses the evolution mechanism as well as the effect of the evolution on the growth of the IMC layer and the mechanical properties.

2. Experimental procedures

SAC solder used in this study was the commercial solder alloy. SACC solder alloy was prepared independently. Alloys used for smelt were pure Sn (99.9%), Ag (99.99%), Cu (99.99%), and Cr (99.99%). The master alloy Sn–2.0Cr was prepared utilizing the vacuum arc furnace for 30 min at ∼1500 °C in high vacuum condition of 1.33×10^{-5} Pa. Then according to the designed composition, Sn–2.0Cr, Ag, Cu, and Sn were sealed into the vacuum quartz tube, which was put into the resistance furnace for 2 h at 1100 °C. Lastly, the alloy was reheated for 1 h at 300 °C and cooled in air.

Solder joint was prepared using the Simulation Preparation Device of Solder Joint. For the substrate, pure copper bars were used and their both ends were polished to remove the surface oxide layer. After fluxing with Kester®Tacky flux, a piece of solder with a diameter of 6 mm and a thickness of 2 mm was emplaced into the thin clearance of the mating surfaces of two copper samples [14]. Subsequently, the whole setting was heated in a temperature-controlled furnace set at 260 ± 5 °C keeping soldering for 5 min, and then cooled in air. The samples were gently pushed towards each other to obtain a good joint.

After joining, the specimens were annealed at 150 °C for 0, 168 and 500 h in an oven. Afterwards, the specimens were cut by electric discharge machining (EDM) and cold mounted in epoxy. To analyze the appearance and evolution of the IMC, they were mechanically ground, polished and etched with a $94\%C_2H_5OH + 4\%HNO_3 + 2\%HCl$ (in vol.%) solution. The microstructure of IMC was observed by means of an Apollo 300 Thermal Field Emission scanning electron microscope (SEM), and the composition was examined by energy dispersive spectroscopy (EDS). The presence of Cr in the solder was detected by transmission electron microscopy (TEM, JSM-2010F) with electron diffraction (ED). A plate sample with a thickness of 1 mm was cut from solder ingot, and ground to about 60 μm. Finally, a disc with a diameter of 3 mm was cut and thinned by an ion-miller for TEM. To study the mechanical properties of solder joints, tensile test was carried out at room temperature at a strain rate of $6.7 \times 10^{-4}\ s^{-1}$ by a CMT5305 tensile tester.

3. Results and discussion

3.1. Microstructure in solder joints

The microstructures of SAC/Cu and SACC/Cu joints after reflow soldering are shown in Fig. 1. The reaction layer on Cu substrate is the scallop-type Cu_6Sn_5 phase in both joints. Besides the interfacial IMC, large IMC can be also seen in the solder. For the SAC/Cu joint, large Cu_6Sn_5 were distributed in the solder, and large needle-like Ag_3Sn formed at the interface of IMC layer. They can be harmful to mechanical integrity of solder joints. In addition, the elongated plate-like Ag_3Sn phases were also present and seen edge-on in SAC solder, as shown in Fig. 1(a). For the SACC/Cu joint, there were also long Cu_6Sn_5 IMC in the solder, but no large Ag_3Sn was observed at the interface, comparing with that for SAC. Plate-like Ag_3Sn were also distributed in the solder and they formed the eutectics together with β-Sn, as shown in Fig. 1(b).

Moreover, a few Sn-rich particles containing Cr, Ag and Cu were formed in SACC/Cu joints, as identified by EDS shown in Fig. 2(a). They couldn't be dissolved in the etching solution, with the structure to be confirmed. The particular particles containing Cr were also found in SACC solder as marked by "1", "2" and "3" in Fig. 2(b), but the content of each element was different from that in SACC/Cu joints. According to the EDS analysis results, the contents of Cr and Cu contained in the particle were increased, while the content of Ag was decreased in SACC/Cu joints, comparing with that in the solder. The content transformation may attribute to the wetting reaction during soldering, which will be illuminated below. Since Cr is almost immiscible with other atoms in this solder joint at room temperature, it may precipitate in the form of particles when the concentration is high enough. To some extent, this assumption is in accord with that Cr dispersed in the solder can pin the boundary and retard the growth of Ag_3Sn and Cu_6Sn_5 compounds, suggested by Zhang et al. [15], although it has not been detected in present work.

3.2. The Ag_3Sn evolution

From the observation of the changes in the microstructure between Fig. 3(a) and (b), it is clear that the large aspect ratio Ag_3Sn plates break up and change into a small aspect ratio (a more circular cross-section) during aging. This is similar to the Ag_3Sn evolution in SAC/Cu joints, as shown in Fig. 3(c) and (d), which is in good agreement with that in SnAgCu and SnAg solder reported by Allen et al. [8] and Shen et al. [9]. They suggested that there were two main mechanisms in the microstructural evolution: plate breakdown due to boundary splitting or a Rayleigh instability and coarsening, and possibly cylinderization of small aspect ratio plates, as well. According to their findings, the breakdown portion is controlled by the interfacial diffusion of tin.

Meanwhile, in present work, some finer Ag_3Sn particles were found rod-shaped and branch-like near the IMC layer of the SACC/Cu joint after soldering, as shown in Fig. 4(a). This can be attributed to the Cr addition and the redistribution of elements with respect to that in the SAC/Cu joint. It is known that the Ag solubility in Cu_6Sn_5 and the Cu solubility in Ag_3Sn are quite small. Likewise for the Cu and Ag solubility in β-Sn in SAC solder [16]. However, in SACC solder, Ag and a small amount of Cu also distribute in some sites which contain Cr in Sn matrix, as described above. During wetting reaction, when temperature increases, the original structure may tend to be unstable. As Cu atoms diffuse into the molten solder, a mass of Sn atoms diffuse to the interface, a few Cu atoms enter the original structure, and Ag atoms migrate to form

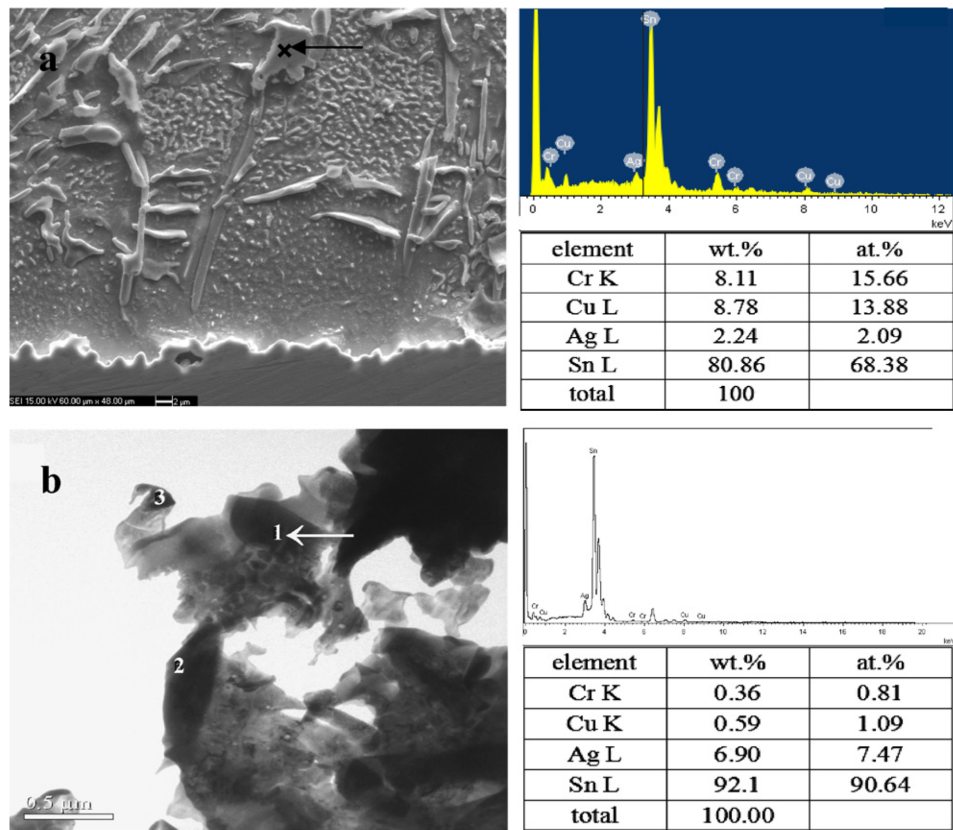

element	wt.%	at.%
Cr K	8.11	15.66
Cu L	8.78	13.88
Ag L	2.24	2.09
Sn L	80.86	68.38
total	100	

element	wt.%	at.%
Cr K	0.36	0.81
Cu K	0.59	1.09
Ag L	6.90	7.47
Sn L	92.1	90.64
total	100.00	

Fig. 2. (a) SEM image of the particle containing Cr in the SACC/Cu joint after reflow soldering; (b) TEM photograph of SACC solder, and EDS analyses of the particles indicated by arrows, respectively.

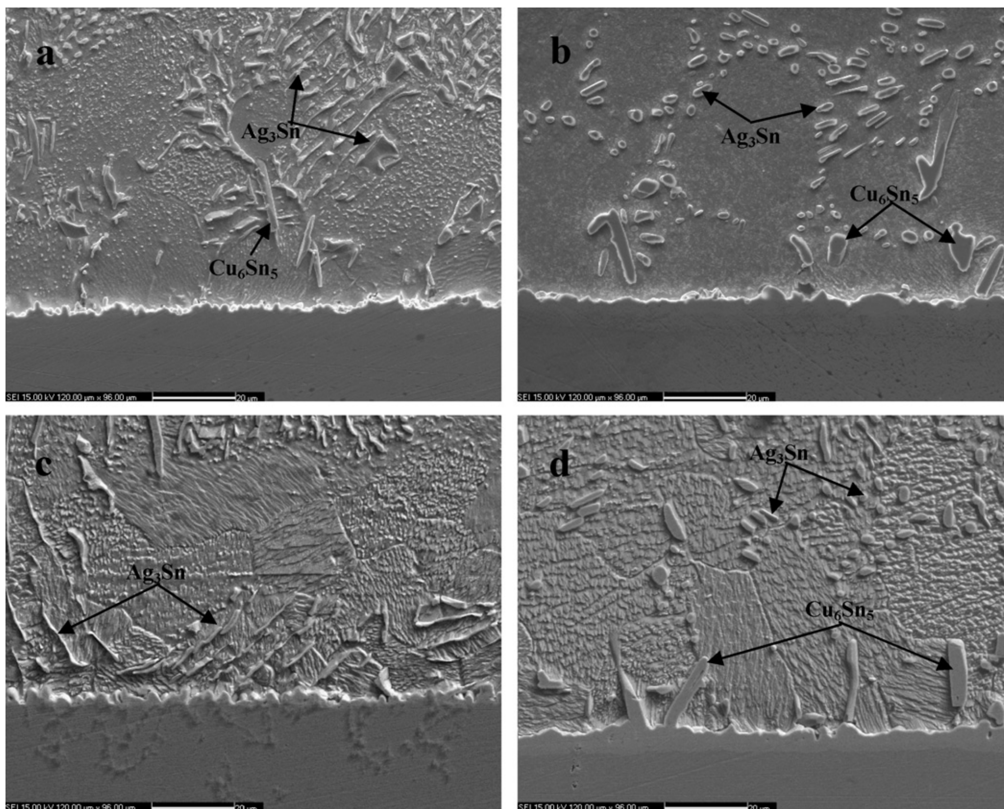

Fig. 3. SEM images of SACC/Cu: (a) as-soldered; (b) after aging for 500 h at 150 °C and SAC/Cu joints: (c) as-soldered; (d) after aging for 500 h at 150 °C.

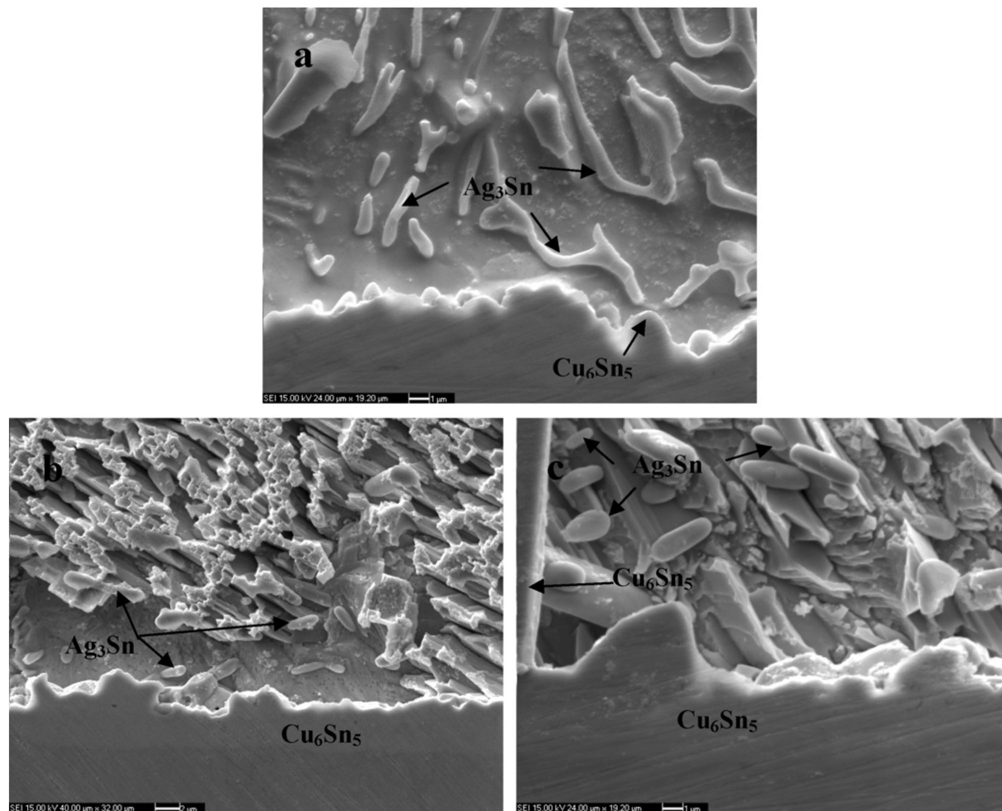

Fig. 4. Morphologies of Ag_3Sn near the SACC/Cu interface: (a) as-soldered; (b) aging for 168 h at 150 °C; (c) aging for 500 h at 150 °C.

finer Ag_3Sn due to the higher affinity between Sn and Ag. Thus, the free energy of the whole system is reduced. It seems that the particles with the presence of Cr promote the nucleation of Ag_3Sn near the IMC layer, which may be due to lowering the standard free energy of the Ag_3Sn formation or providing more heterogeneous nucleation. This hypothesis needs further study and confirmation.

During thermal aging at 150 °C, morphologies of Ag_3Sn near the interfacial layer of SACC/Cu joint were different at different stages, as indicated by the arrows (Fig. 4). After isothermal aging for 168 h, the long Ag_3Sn with rough surface and different diameters along the length (Fig. 4(a)) became short and the surface was relatively smooth, as shown in Fig. 4(b). When the aging time extended to 500 h, much shorter Ag_3Sn rods or small ellipsoidal Ag_3Sn particles were found near the interface of IMC layer, as shown in Fig. 4(c). The ends of Ag_3Sn particles became rounded and some small particles were even found on the top of IMC layer. In the cases of SAC/Cu joints, the morphology of Ag_3Sn near the IMC interface has no such obvious change as that in SACC/Cu joints. So it is expected that the addition of Cr has effect on the morphology change of Ag_3Sn.

Zhu et al. [17] found that the large needle-shaped Ag_3Sn were refined into small particles and evenly distributed in Sn3.8Ag0.7Cu solder alloy after equal channel angle pressing process and long-term aging. Zeng et al. [18] also have reported that thin rod-shaped Ag_3Sn became shorter and coarser, and their ends became more rounded in Sn3.5Ag2Bi alloy, due to the recrystallization after absorbing ample interfacial energy during indentation creep at 90 °C. They both applied external mechanical stress on the solder alloy and a large number of excess vacancies were produced at the phase interface under local static stress, which enhanced the atomic diffusion along the interface. In addition, the interfacial energy also increased during the pressing process. Thus, the morphology evolution of Ag_3Sn occurred. Allen et al. [8] also provided a detailed explanation for breakdown of plate-like Ag_3Sn in the solder alloy. However, in present work, without external stress applied, the SACC/Cu joints were only treated by isothermal aging at 150 °C, and the Ag_3Sn particles near the IMC interface became shorter and changed to small ellipsoidal particles spontaneously.

Since the driving force for spheroidization is the reduction of total energy, to analyze the morphological evolution of these Ag_3Sn particles, a schematic diagram is present, as shown in Fig. 5. The diameter of the original Ag_3Sn along the length is not always the same, which may lead to boundary and composition instability of local sections. So it can be inferred that the diameter fluctuation may lead to Rayleigh-type instability. From the data in Table 1 according to Ref. [8], it can be seen that the activation energies for Sn and Ag volume diffusion are too high, so the interfacial diffusion may be rate controlling mechanism for spheroidization. During aging at 150 °C, the vibrational energy and diffusion coefficient of atoms increase, so do vacancies in solder matrix. Although the extremely small solid solubility of Ag in β-Sn limits its diffusion, a mass of defects (e.g. dislocations and vacancies) at the phase

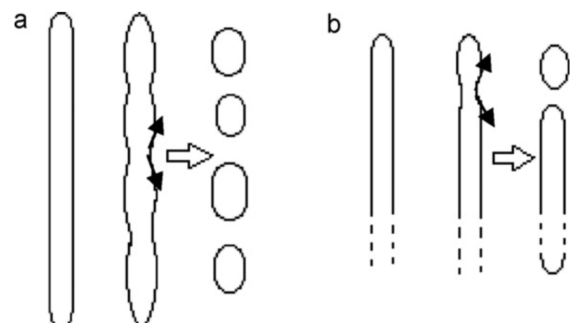

Fig. 5. Schematic diagrams of evolution of Ag_3Sn particles.

Table 1
Literature values of activation energies for diffusion (D) of silver, copper, and tin in tin, and the heats of solution (S) of silver and copper in tin. Also provided are activation energies for grain boundary diffusion of silver and tin in tin.

Element	In	Q (kJ mol^{-1})
Ag	Sn (c-axis)	55(D)
Ag	Sn (a-axis)	77(D)
Sn	Sn (c-axis)	107(D)
Sn	Sn (a-axis)	123(D)
Ag	Sn grain boundaries	28(D)
Sn	Sn grain boundaries	40(D)
Ag	Sn	26(S)

interface enhance the diffusion of Ag atoms along the interface. Table 1 shows the activation energy for diffusion of Ag along Sn grain boundaries is 28 kJ mol^{-1}, which is lower than that for Sn (40 kJ mol^{-1}). So it is possible to say that the spheroidization process is controlled by the interfacial diffusion of Ag, though attempts to measure data for diffusion of Ag and Sn along Ag_3Sn/β-Sn interfaces meet with little success in this work.

Therefore, it is inferred that the Ag_3Sn/β-Sn interface plays a very important role in the morphological evolution of Ag_3Sn. Ag atoms may break away from the Ag_3Sn lattice at the interface of local sections with smaller diameter due to the interfacial tension. Then, they diffuse along the Ag_3Sn/β-Sn interface into the Sn lattice and form new Ag_3Sn, as revealed by the arrows in Fig. 5. Gradually, the concave section may become deeper, break down and finally

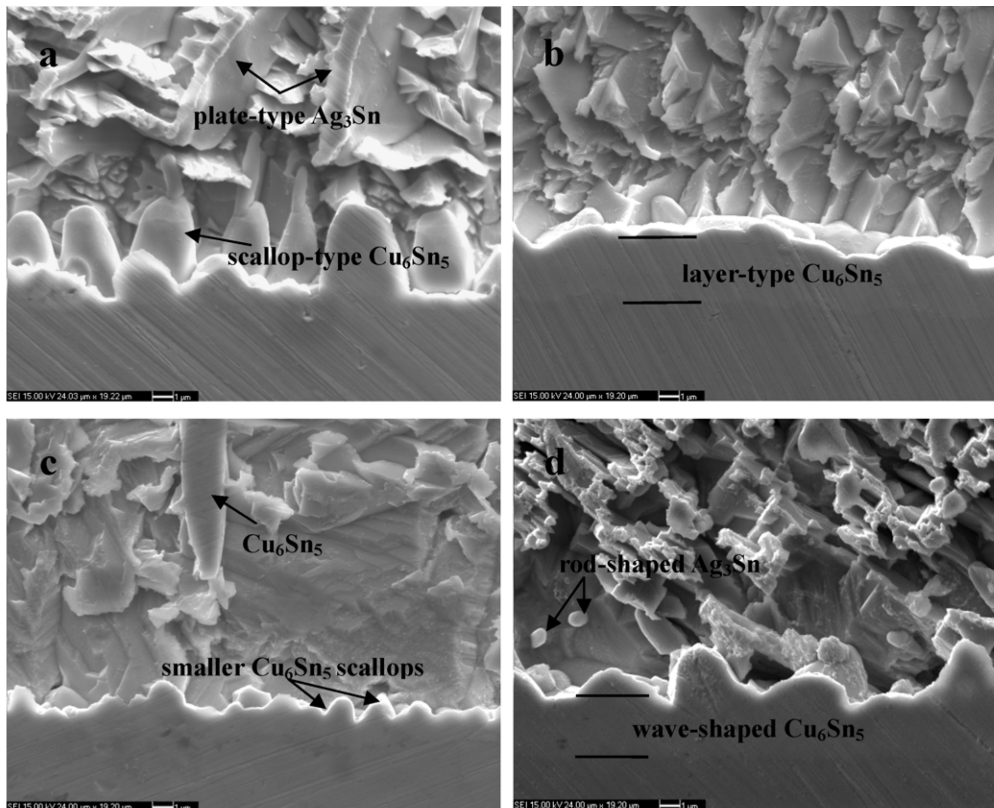

Fig. 6. Cross-sectional SEM images of IMC layers of SAC/Cu joints: (a) as-soldered; (b) after aging for 168 h at 150 °C and SACC/Cu joints: (c) as-soldered; (d) after aging for 168 h at 150 °C.

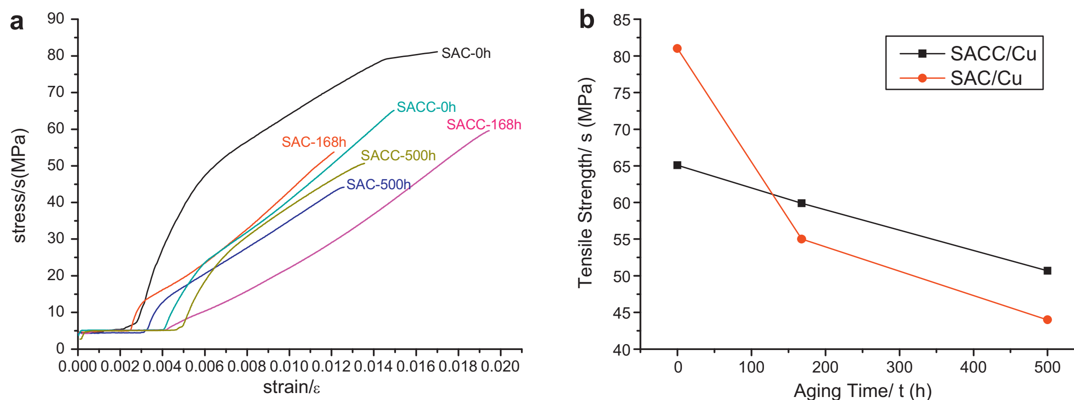

Fig. 7. The stress–strain curves (a) and strength-aging time curves (b) for the two joints after aging at 150 °C.

shrink into rounded ends of particles. Thus, the long Ag_3Sn divides into several particles. The evolution process and the space between the near-spherical particles depend on the interfacial tension and diffusion coefficient. If the original Ag_3Sn is long enough, it may change into a string of near-spherical particles (Fig. 5(a)); if the ratio of length and diameter of Ag_3Sn rod is appropriate, it may change into a spherical particle and a shorter rod, which may continue to evolve (Fig. 5(b)). In conclusion, from the viewpoint of surface free energy, to minimize the interfacial free energy, the local section of Ag_3Sn with smaller diameter has to break down and shrink into near-spherical particles. So the total interfacial area becomes smaller and the entire system free energy reduces.

Moreover, the redistribution of elements during aging may also promote the evolution of Ag_3Sn. Atom diffusion is much faster at 150 °C than that at room temperature. As the interfacial reaction is weakened due to the Cr addition, the excessive Sn at the interface is discharged into the matrix, resulting in uphill diffusion. The redistribution of elements and diffusion may cause destruction of the interface balance of Ag_3Sn. To reach new balance, the sharp corners of Ag_3Sn with small radius of curvature dissolve and shrink. Thus, the long Ag_3Sn changes to shorter and small ellipsoidal particles.

3.3. The IMC layer and tensile properties of joints

Fig. 6 shows the cross-sectional images of the SAC/Cu and SACC/Cu joint interfaces. A much clearer three-dimensional image of scallop-type Cu_6Sn_5 is revealed in the SAC/Cu joint. The scallops are separated by channels whose depth almost reaches the Cu surface. And the plate-type Ag_3Sn forms in the solder near the interface, as shown in Fig. 6(a). During the subsequent thermal aging, the scallops grow together, the channels disappear and the morphology of IMC growth is layer-type. By comparison, the scallops are much smaller in the SACC/Cu joint just after soldering. The morphology of IMC growth is regular wave-shape and the thickness is even during thermal aging. The Ag_3Sn IMC formed near the IMC layer are rod-shaped and branch-like, as shown in Figs. 6(d) and 4(a).

The trace Cr addition observably affected the growth rate and shape of IMC layer at the interface of solder joint, though scarcely affected the IMC composition. In our previous study [13], the diffusion coefficients of IMC layers at the interface of SACC/Cu and SAC/Cu joints were $3.90 \times 10^{-18}\,m^2\,s^{-1}$ and $1.16 \times 10^{-17}\,m^2\,s^{-1}$, respectively. It should be noted that the IMC layer of the SACC/Cu joint is extraordinarily thin after soldering. The reason for the fast interfacial reaction in SAC system is that Cu diffuses in Sn due to higher composition gradient. So the activity of Sn is a decisive factor governing the interfacial diffusion kinetics. Previous study [15] suggested that Cr dispersed in the solder could pin the boundary and retard the growth of Ag_3Sn and Cu_6Sn_5 compounds. Present research indicates that the dispersion of Cr with Ag and Cu in Sn matrix holds Sn atoms and reduces diffusion coefficient of Sn and Cu. Furthermore, a portion of Cu atoms diffusing to the solder may enter the sites with Cr, forming a new special phase to be identified. So the Cr in Sn matrix weakens the reaction rate of Sn and Cu, reducing the growth rate of the IMC layer. This may be the important reason that a thin IMC layer forms in the SACC/Cu joint during soldering.

It is well known that high bonding strength of the joint interface largely depends on appropriate thickness of the IMC layer and morphology of the interface. For as-soldered joints, the very thin IMC layer is the crucial factor in lower bonding strength of SACC/Cu joint compared with that of SAC/Cu whose scallop-type Cu_6Sn_5 IMC layer embedded in the solder matrix provides a higher bonding strength, as shown in Fig. 7. After aging for 168 h at 150 °C, the wave-shaped IMC layer of SACC/Cu joint grows more slowly to an appropriate thickness, maintaining a relative high bonding strength; the layer-type IMC layer in SAC/Cu joint grows too fast, resulting in rapid decline of strength (Fig. 7(b)).

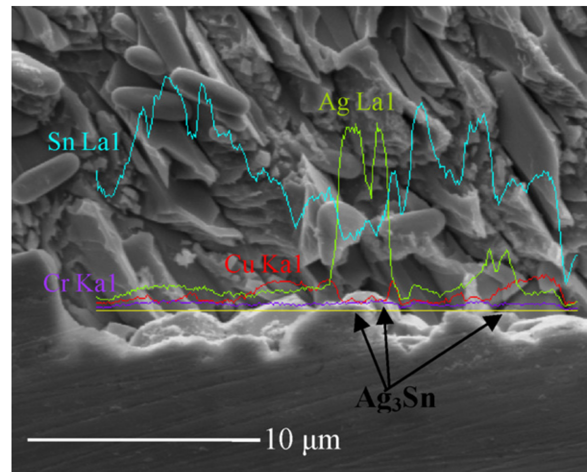

Fig. 8. Ag_3Sn particles on the IMC layer of the SACC/Cu joint after aging for 500 h at 150 °C.

After aging for 500 h at 150 °C, small Ag_3Sn particles with the size of about 1 μm were found on the IMC layer, as revealed in Fig. 8. It is known that some Ag_3Sn particles are embedded within the Cu_6Sn_5 layer during long-term aging related to the depletion of Sn close to the IMC layer in SnAg/Cu and SnAgCu/Cu joints [10,19]. Here, with much shorter aging time, the Ag_3Sn particles seem to be on the top of the IMC layer. According to Yu et al. [10], these particles may be attributed to the growing up of smaller Ag_3Sn by a ripening process during aging. Because of the dispersion of Cr with Ag and Cu in Sn matrix and the higher affinity between Sn and Ag, there may be not only short-range order (SRO) Ag_3Sn groups but also medium-range order (MRO) Ag_3Sn groups in the liquid solder at the soldering temperature. So it can be deduced that smaller Ag_3Sn particles would form on the IMC layer in SACC/Cu joint during soldering. Their existence can suppress the growth of IMC layer during both soldering and aging, due to decreasing the surface energy of the layer. That may be one of the reasons for the thinner wave-shaped IMC layer, which greatly contributes to maintaining a better strength for SACC/Cu joint during thermal aging, compared with SAC/Cu, as Fig. 7(b) shows.

Forming shorter rod-shaped and near-spherical Ag_3Sn particles, the Ag_3Sn evolution near IMC layer and the thinner wave-shaped IMC layer make a great contribution to the strength and elongation of joints against thermal aging. This can be confirmed by Fig. 7(a), from which the tensile strength and elongation of SACC/Cu joints are obviously superior to that of SAC/Cu after aging for 168 h and 500 h, though the property of the latter is higher just after soldering. Consequently, the favorable morphology of joint interface leads to better bonding properties for SACC/Cu joint than that for SAC/Cu joint against thermal aging.

4. Conclusions

Different shaped Ag_3Sn particles were found in the Sn matrix and near the IMC layer in SACC/Cu joints after soldering and aging:

(1) Plate-like Ag_3Sn were distributed in the solder matrix of joints, while finer rod-shaped and branch-like Ag_3Sn were present near the interface of IMC layer after soldering. Cr present with Ag and Cu in Sn matrix may promote the nucleation of Ag_3Sn, forming the finer Ag_3Sn.
(2) Long Ag_3Sn changed into shorter rods and small particles near the interface during aging at 150 °C. Diffusion of Ag along the

Ag_3Sn/β-Sn interface and the redistribution of elements due to slow growth of IMC layer may result in breakdown and shrinkage of the local section of Ag_3Sn with smaller diameter, forming shorter rods and near-spherical Ag_3Sn particles. In the evolution process, the interfacial free energy tends to minimize.

With the thinner wave-shaped IMC layer and smaller near-spherical Ag_3Sn particles, the favorable morphology of joint interface leads to better bonding properties for SACC/Cu joint than that for SAC/Cu against thermal aging.

Acknowledgments

The present work was carried out with the support of the Foundation for Innovation in Shanghai University (contract No. SHUCX102232), the Special Foundation for Outstanding Young Teachers in Shanghai University (contract No. B.37-0209-09-001) and Open Foundation of Key State Lab for New Displays and System Integration (Chinese Ministry of Education).

References

[1] M. Abtew, G. Selvaduray, Mater. Sci. Eng. R 27 (2000) 95–141.
[2] E. Saiz, C.W. Hwang, K. Suganuma, A.P. Tomsia, Acta Mater. 51 (2003) 3185–3197.
[3] K.N. Yu, A.M. Gusak, M. Li, J. Appl. Phys. 93 (2003) 1335–1353.
[4] K.S. Kim, S.H. Huh, K. Suganuma, J. Alloys Compd. 352 (2003) 226–236.
[5] H.T. Lee, Y.F. Chen, J. Alloys Compd. 509 (2011) 2510–2517.
[6] L.G. Liljestrand, L.O. Anderson, Circuit World 14 (1988) 3.
[7] P. Sun, C. Andersson, X. Wei, Z. Cheng, D. Shangguan, J. Liu, Mater. Sci. Eng. B 135 (2006) 134–140.
[8] S.L. Allen, M.R. Notis, R.R. Chromik, R.P. Vinci, J. Mater. Res. 19 (2004) 1425–1431.
[9] J. Shen, Y. Liu, H. Gao, Chin. Sci. Bull. 51 (2006) 1766–1770.
[10] D.Q. Yu, L. Wang, C.M.L. Wu, C.M.T. Law, J. Alloys Compd. 389 (2005) 153–158.
[11] X.Y. Liu, M.L. Huang, Y.H. Zhao, C.M.L. Wu, L. Wang, J. Alloys Compd. 492 (2010) 433–438.
[12] L.C. Tscao, J. Alloys Compd. 509 (2011) 2326–2333.
[13] G. Su, Y. Han, C. Wang, H. Wang, X. Wei, Proceedings of the 16th IEEE International Symposium on the Physical and Failure Analysis of Integrated Circuits, 2009, pp. 393–396.
[14] G. Ju, X. Wei, J. Liu, Solder. Surf. Mt. Technol. 20 (2008) 4–10.
[15] F. Zhang, J. Liu, F. Yang, Q. Hu, H. He, X. Zhu, J. Xu, L. Shi, Electron. Comp. Mater. 24 (2005) 45–48.
[16] K.W. Moon, W.J. Boettinger, U.R. Kattner, F.S. Biancaniello, C.A. Handwerker, J. Electron. Mater. 29 (2000) 1122–1136.
[17] Q. Zhu, L. Zhang, Z. Wang, S. Wu, J. Shang, Acta Metall. Sin. 43 (2007) 41–46.
[18] M. Zeng, Z. Chen, B. Shen, D. Xu, Chin. J. Nonferr. Met. 18 (2008) 620–625.
[19] S. Choi, T.R. Bieler, J.P. Lucas, K.N. Subramanian, J. Electron. Mater. 28 (1999) 1209–1215.